Robust regeneration of adult zebrafish lateral line hair cells reflects continued precursor pool maintenance

Ivan A. Cruz [a,b], Ryan Kappedal [c], Scott M. Mackenzie [b,d], Dale W. Hailey [b],
Trevor L. Hoffman [e,f], Thomas F. Schilling [e], David W. Raible [a,b,d,*]

[a] Molecular Cellular Biology Graduate Program, University of Washington, Seattle, WA 98195, USA
[b] Department of Biological Structure, University of Washington, Seattle, WA 98195, USA
[c] Department of Statistics, University of Washington, Seattle, WA 98195, USA
[d] Neurobiology and Behavior Graduate Program, University of Washington, Seattle, WA 98195, USA
[e] Department of Developmental and Cell Biology, University of California, Irvine, CA 92697-2300, USA
[f] Kaiser Permanente, 5971 Venice Boulevard, West Los Angeles, CA 90034, USA

ARTICLE INFO

ABSTRACT

We have examined lateral line hair cell and support cell maintenance in adult zebrafish when growth is largely complete. We demonstrate that adult zebrafish not only replenish hair cells after a single instance of hair cell damage, but also maintain hair cells and support cells after multiple rounds of damage and regeneration. We find that hair cells undergo continuous turnover in adult zebrafish in the absence of damage. We identify mitotically-distinct support cell populations and show that hair cells regenerate from underlying support cells in a region-specific manner. Our results demonstrate that there are two distinct support cell populations in the lateral line, which may help explain why zebrafish hair cell regeneration is extremely robust, retained throughout life, and potentially unlimited in regenerative capacity.

© 2015 Elsevier Inc. All rights reserved.

Introduction

The phenomenon of regeneration allows multicellular organisms to restore lost or damaged structures. The robustness and degree of such processes depend on numerous factors, including tissue location, age and species (see Rando and Wyss-Coray (2014), Sousounis et al. (2014) for reviews). Humans and other mammals have restricted regenerative ability that becomes progressively more limited with age. A few tissues in mammals can regenerate robustly well into late age and after drastic trauma (e.g. blood, skin, and intestinal epithelia). These tissues are exposed to environmental insults that cause accumulation of acute damage over time, undergo continuous cellular loss and replacement, and have dedicated progenitor cells sequestered in distinct locations (reviewed in Barker et al. (2010) and Tetteh et al. (2014)). However, some cell types, like mechanosensory hair cells located in the sensory epithelia of the adult mammalian ear, show little or no regeneration after age-related and/or trauma-induced hair cell death, which leads to permanent hearing and balance disorders (Hawkins and Atha, 1976; Raphael et al., 1991; Brigande and Heller,

2009). Non-mammalian vertebrates, such as salamanders and zebrafish, have the remarkable ability to regenerate a wide range of tissues, including limbs, heart, and spinal cord (see Gemberling et al. (2013), Simona and Tanaka (2013), and Fior (2014) for reviews).

Zebrafish (Danio rerio) have hair cells that are structurally and functionally similar to mammalian hair cells (Whitfield, 2002; Nicolson, 2005). In addition to hair cells within the inner ear, zebrafish have hair cells within the lateral line system, a sensory system that detects water fluctuations with externally-located sensory organs called neuromasts. Neuromasts are composed of centrally-positioned mechanosensory hair cells surrounded by non-sensory support cells (see Thomas et al. (2015) for review). Exposure to clinical therapeutic drugs such as aminoglycoside antibiotics that induce hair cell death within the mammalian inner ear also rapidly induce hair cell death in the lateral line system (Song et al., 1995; Harris et al., 2003; Ton and Parng, 2005; Ou et al., 2007). However, unlike their mammalian counterparts, zebrafish have retained the ability to regenerate hair cells after damage (Williams and Holder, 2000; Harris et al., 2003; López-Schier and Hudspeth, 2006; Hernández et al., 2007; Ma et al., 2008; Wibowo et al., 2011; Pisano et al., 2014).

It is unknown to what degree zebrafish neuromasts maintain hair cells and support cells under different environmental conditions

* Corresponding author at: Department of Biological Structure, University of Washington, Seattle, WA 98195, USA.
E-mail address: draible@uw.edu (D.W. Raible).
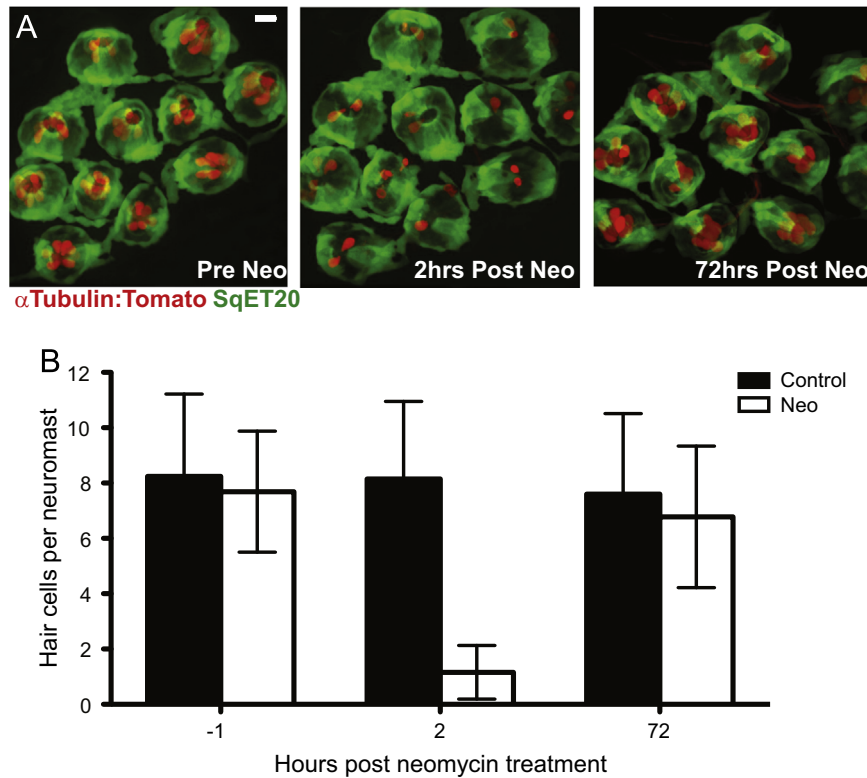
Fig. 1. Adult zebrafish lateral line hair cell regeneration after neomycin-induced ablation. Confocal z-stack maximum projection images of a peduncle stitch (11 neuromasts) of an adult *sqet20Et;Tg(Ca-tuba1a:tdTomato)* zebrafish with hair cells labeled with tdTomato (red) and a subset of support cells labeled with GFP (green). (A) Adult zebrafish peduncle neuromasts (left panel) were treated with 400 μM neomycin for 1 h (middle panel) and then allowed to recover for 72 h to assess hair cell regeneration (right panel). (B) Results are graphed as average number of hair cells per neuromast (± s.d.) for each treatment group. $N=4$ adult zebrafish per group, 40+ neuromasts per group. Scale bar, 10 μm.

throughout the animal's lifetime. It has been previously demonstrated in larval fish lateral line that terminally differentiated hair cells regenerate from symmetric divisions of underlying support cells (López-Schier and Hudspeth, 2006; Wibowo et al., 2011) and there is evidence to suggest that larval hair cells undergo turnover (Williams and Holder, 2000). However, continuous hair cell production from symmetrically dividing support cells would eventually deplete a hair cell precursor population. Given the relatively small number of larval support cells per neuromast, current models fail to account adequately for either turnover or neuromast growth through larval development into adulthood.

Using transgenic zebrafish, we analyzed the functions of different support cell populations within the zebrafish lateral line system during hair cell regeneration. Here we demonstrate that not only adult zebrafish regenerate hair cells following ototoxin-induced damage, but also they can regenerate hair cells after multiple iterations of damage, well into old age. We show that under ambient conditions there is a constant loss and replacement of hair cells. Fate mapping studies reveal distinct precursors within neuromasts. Our results indicate that zebrafish lateral line hair cells have a largely unlimited regenerative ability that is retained into adulthood, and that at least two different support cell populations exist to maintain tissue integrity within the lateral line system.
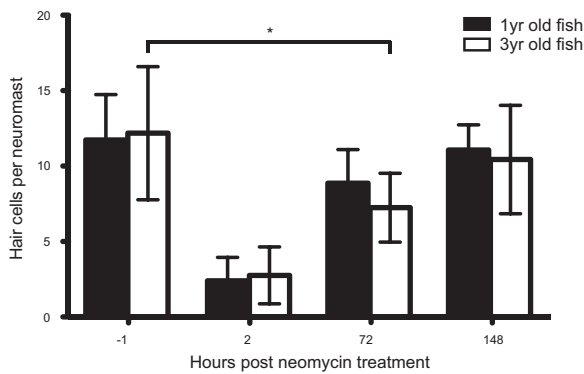
Results

Adult zebrafish regenerate posterior lateral line hair cells after neo-mycin-induced hair cell ablation

As previous studies have mostly focused on larval zebrafish, we wanted to investigate hair cell regeneration following damage in mature adults. We examined the regenerative ability of sexually mature adult zebrafish using a transgenic line *Ca-tuba1a:tdTomato*, which labels all mature hair cells with the red fluorescent protein *tdTomato*, and *sqet20Et,* an enhancer trap line that labels a subset of support cells with GFP and therefore serves as a convenient landmark for neuromast position when hair cells are missing (Fig. 1A). Hair cell numbers were counted within all neuromasts of the most posterior stitches of the trunk peduncle, 1 h before, and both 2 and 72 h after neomycin treatment (Fig. 1A). Following neomycin exposure the average number of hair cells per neuromast dropped by more than 75% after 2 h but then returned to pre-treatment numbers after 72 h of recovery in drug-free media (Fig. 1B). This rate of recovery is similar to previous reports examining hair cell regeneration and maturation in larval zebrafish (Ma et al., 2008; Mackenzie and Raible, 2012). These results indicate that lateral line hair cell regeneration is not developmentally limited, and that it is maintained in neuromasts of adult zebrafish.

Hair cell regeneration is complete in the lateral line system of aged zebrafish

We next determined whether regenerative capacity is lost with age. We compared hair cell replacement in adult 1-year-old zebrafish and 3-year-old zebrafish using the same damage method and transgenic fish as used for the previous experiment (Fig. 2). We found that 3-year-old fish regenerated hair cells, completely restoring hair cell numbers. In contrast to younger adults, hair cell replacement took longer, and was not complete until 5 days after damage compared to 3 days in younger animals. Nevertheless, senescent zebrafish are able to fully replace hair cells lost after neomycin treatment.

Fig. 2. Lateral line hair cell regeneration of senescent adult zebrafish following hair cell death. 1 year and 3 year old zebrafish were treated with 400 μM neomycin for 1 h and then allowed to recover for 72 h. The results are graphed as average number of hair cells per neuromast ($\pm$ s.d.) for each treatment group. $N=3$ adult zebrafish per group, 20+ neuromasts per group; $p < 0.001$ (ANOVA posthoc test).
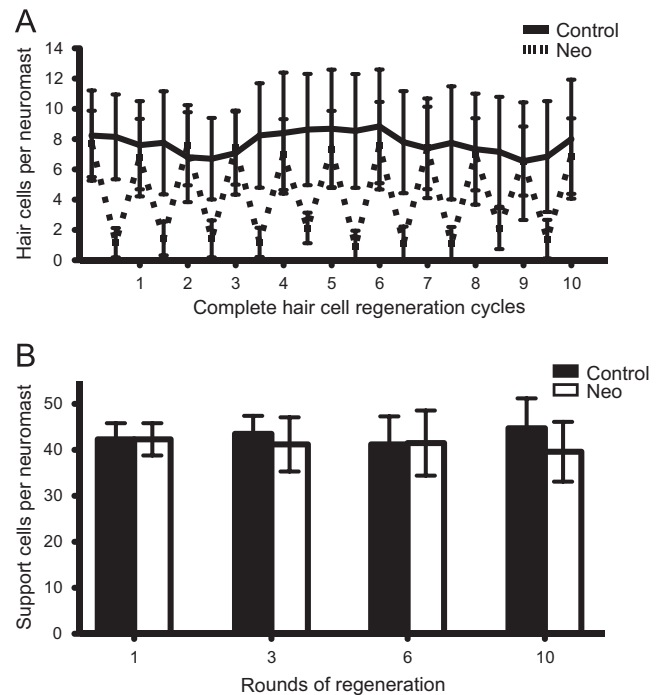
Hair cells regenerate after multiple iterations of damage

We investigated the regenerative robustness and maintenance of hair cells and support cells after multiple rounds of neomycin damage. The same cohort of fish was followed through 10 sequential rounds of hair cell ablation and regeneration (Fig. 3A). Similar to the single regeneration paradigm, most hair cells were lost 2 h after neomycin exposure, and subsequently replaced during the recovery period following each treatment iteration. This experiment illustrates that lateral line hair cell regeneration is responsive and robust over many repeated insults.

Hair cells in larval zebrafish are generated from symmetrically dividing support cell precursors, suggesting that their differentiation would result in depletion of hair cell precursors. We therefore assessed whether there were changes in support cell numbers with repeated rounds of hair cell loss in adults. Adult *Tg (pou4f3:gap43-GFP)* zebrafish, which label hair cells with GFP, were collected, fixed, and stained with pan-nuclear stain Sytox Green to identify support cells (Ma et al., 2008). Support cells were quantified and averaged after 1, 3, 6, and 10 sequential neomycin treatments (Fig. 3B). Only after 10 treatments did we observe a small but significant difference between the average numbers of support cells per neuromast in the treated group compared to the control. All other neomycin treated groups showed no difference when compared to their respective controls (two way-ANOVA, p-value > 0.05). The preservation of support cells and hair cells following 10 neomycin treatments suggests that support cell renewal is tightly regulated during hair cell regeneration.

Continuous hair cell loss and replacement occurs in the adult zebrafish lateral line

Regenerative tissues such as skin or intestine also exhibit cellular turnover to replace old cells that may have accumulated damage over time. We wanted to establish whether zebrafish lateral line hair cells are continuously lost and replaced in adult animals. We labeled a cohort of hair cells by first treating *pou4f3:gap43-GFP* transgenic fish and allowing regeneration to occur in the presence of BrdU to label newly regenerated hair cells. Label retention was then assessed over time under ambient conditions (Fig. 4A, diagram). GFP+ and BrdU+ hair cells were quantified for all the neuromasts in the posterior peduncle stitches at 2, 6, and 12 days after BrdU incorporation (Fig. 4B, left, center, right panels, respectively). Slightly, over half of the hair cells per neuromast were positive for both GFP and BrdU 2 days post-treatment. We found that the percentage of BrdU+ hair cells decreased following 6 and 12 days post-BrdU exposure, while at the same time the total number of hair cells remained unchanged

Fig. 3. Hair cell and support cell regeneration in adult zebrafish after multiple sequential neomycin treatments. (A) Adult *sqet20Et;Tg(Ca-tuba1a:tdTomato)* zebrafish were treated with 400 μM neomycin and allowed to recover for 10 sequential neomycin-induced hair cell destruction/regeneration cycles. For each cycle hair cells were allowed to regenerate for 72 h. We allowed an extra 24 h of recovery after the 9th neomycin treatment to have hair cells numbers surpass 85% of the previous hair cell quantification. Results are graphed as average number of hair cells per neuromast ($\pm$ s.d.) for each treatment group. $N=4$ adult zebrafish per group, 40+ neuromasts per group. (B) Support cell averages were quantified from adult *Tg(pou4f3:gap43-GFP)* zebrafish that were neomycin treated 1, 3, 6, and 10 sequential times, euthanized, and stained with the pan-nuclear stain Sytox Green after each indicated neomycin treatment. Results were graphed as support cell averages per neuromast ($\pm$ s.d.) for each treatment group. $N=3$–4 adult zebrafish per group, 15+ neuromasts per group.

(Fig. 4C). These results suggest that adult lateral line hair cells regenerate through mitotic divisions and are lost and replaced over time under non-traumatic conditions.

We also monitored live turnover of lateral line hair cells using the transgenic line, *myo6b:NLS-Eos*, which labels lateral line hair cell nuclei with the photoactivatable fluorescent protein Eos. Under normal conditions Eos fluoresces green (Fig. 5A, left panel), but when briefly exposed to 405 nm UV light, the protein undergoes an irreversible conformational change to permanently fluoresce red (Fig. 5A center panel). Eos in hair cells of the peduncle stitches of adult *Tg(myo6b:NLS-Eos)* fish was photoconverted to the red conformation, and persistence of red-labeled cells was monitored over time. "Old" hair cells containing elevated levels of red fluorescence were present at the time of 405 nm laser photoactivation (Fig. 5A, arrowhead right panel), and "new" hair cells that did not have elevated levels of red fluorescence were hair cells generated after the photoactivation (Fig. 5A, arrow right panel). We note that both old and new hair cells express green Eos as photoconverted cells continue to make new protein. Immediately after UV exposure, all hair cells had elevated red fluorescence compared to non-converted controls. Over time, the average number of old hair cells slowly decreased, but the loss of old hair cells was complemented by the production of new hair cells (Fig. 5B, dotted lines). There was little loss of red fluorescence in cells that remain over the time course of the experiment. This is not surprising since we have observed retention of high fluorescence levels of red nuclear-Eos persisting for months following photoconversion. This experiment indicates that neuromasts
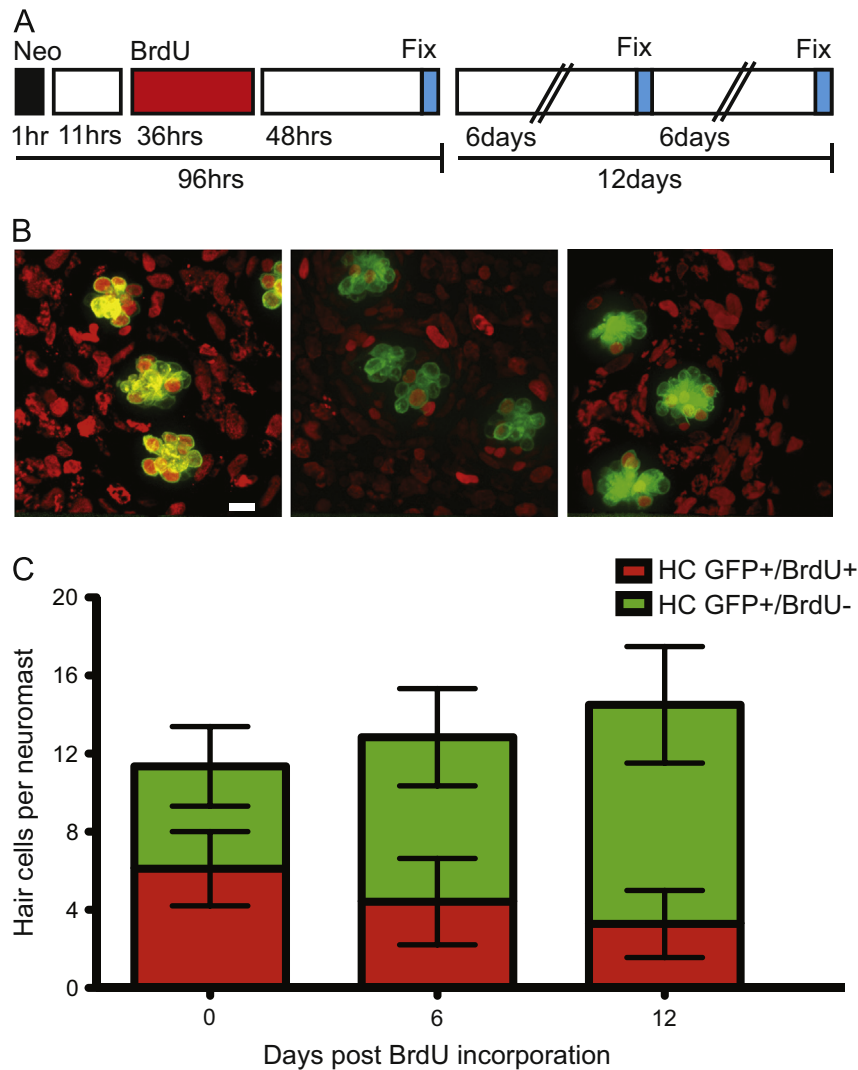
Fig. 4. In adult zebrafish, BrdU labeled lateral line hair cells are lost over time under ambient conditions. (A) Schematic illustrating the experimental protocol: fish were treated with 400 μM neomycin for 1 h, then allowed to recover for 11 h, followed by a 36 h 5 mM BrdU incubation period, and finally fixed and stained at the indicated time-points. (B) Representative confocal z-stack maximum intensity projection images of neuromasts with hair cells labeled green with GFP and BrdU positive cell nuclei marked red. BrdU+ hair cells 0 days (left panel), 6 days (middle panel), and 12 days (right panel) after hair cell regeneration. Scale bar, 10 μM (C) Graph illustrating stacked averages (± s.d.) of GFP+ only hair cells (green) and GFP+ hair cells co-labeled with BrdU (red). $N=2-3$ adult zebrafish per condition, 30+ neuromasts per group.

continuously lose and replace hair cells under ambient conditions and maintain a consistent number of hair cells over time.

To investigate whether the continuous loss of hair cells reflects a cell intrinsic clock regulating lifespan, hair cells were temporally synchronized by first killing with neomycin. Newly regenerated hair cells were then marked by Eos photoconversion, and hair cell loss was then monitored over time (Fig. 5B, solid lines and dotted lines, respectively). There was no difference in the average number of old or new hair cells present 18 days post-photoactivation between synchronized and unsynchronized neuromasts, or in the rate of loss over the experimental period. These results suggest that hair cells do not have an internally calibrated schedule of senescence.

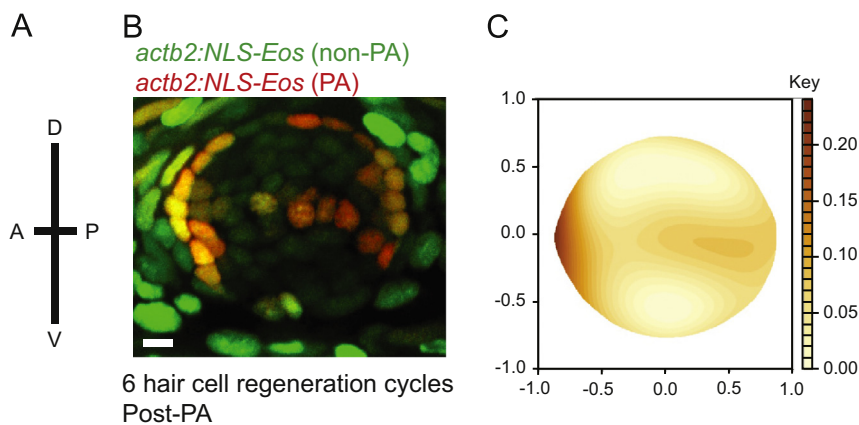*Label retaining support cells are localized at the anterior pole of neuromasts*

A heterogeneous support cell population within zebrafish neuro-masts could explain how hair cells are produced from symmetrically dividing support cells while retaining support cell numbers through multiple rounds of hair cell regeneration. Dedicated long-lived and self-replenishing support cell progenitors could replace and maintain hair cell precursors. A common method of differentiating mitotically

distinct cell populations is through label retention using a pulse-chase assay. We attempted to identify distinct support cell populations based on differential turnover using a transgenic fish line *actb2:NLS-Eos*, which expresses nuclear localized Eos in all support cells. Caudal fin neuromasts were used for this experiment because phalloidin labeling showed that the polarities of the hair cells of these neuromasts are all oriented along the anterior–posterior axis (IAC, unpublished results). We expected after multiple rounds of induced regeneration that multiple cell divisions would dilute the red Eos present in dividing support cells that give rise to hair cells, while support cells that did not divide or that divided less frequently would retain higher levels of the red Eos protein. To have a common frame of reference, individual neuromast shapes were warped and normalized in order to aggregate data of all neuromasts together to a single standardized model (see Supplemental text).

Eos was photoconverted in all support cells of neuromasts in the adult zebrafish caudal fin, and fish were then subjected to 5 sequential neomycin treatments separated by recovery periods to allow hair cells to regenerate. We found a large primary population of label-retaining support cells at the anterior end of the neuromast, and more variably a smaller secondary popula-tion was located at the posterior end of neuromasts. The dorsal
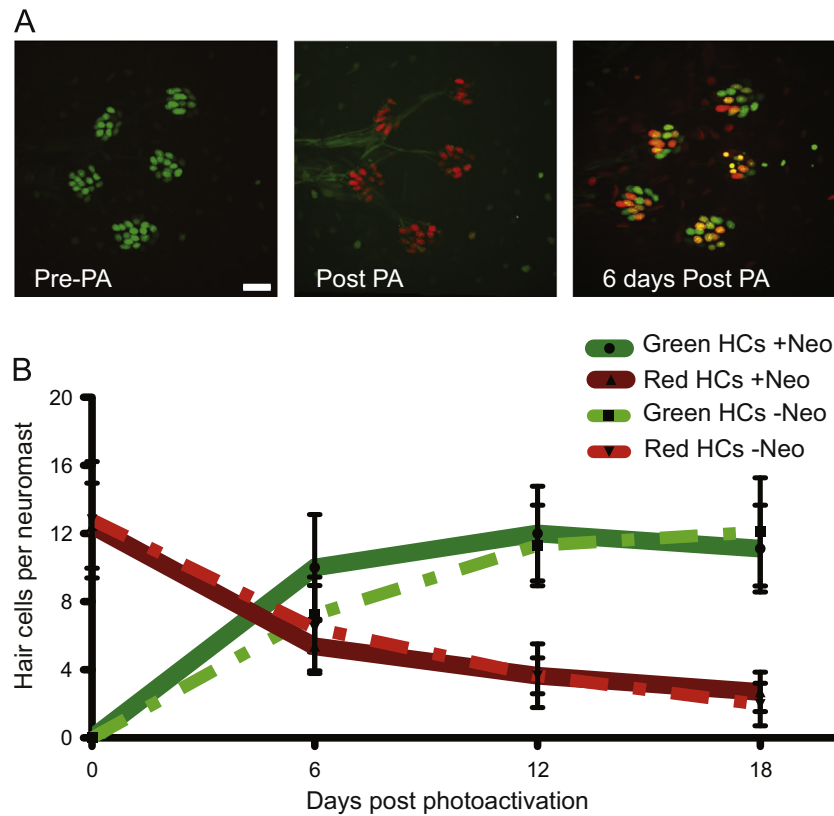
Fig. 5. Hair cells are continuously lost and replaced in adult zebrafish lateral line. (A) Representative z-stack confocal maximum projection images of an adult *Tg(myo6b:NLS-Eos)* peduncle stitch (5 neuromasts shown) before photo-activation, or PA (left panel), immediately after PA (middle panel), and 6 days after PA (right panel). Because Eos is under the control of the *myo6b* promoter, green Eos is continuously produced therefore hair cells that were present at the time of photo-activation will have both green and red Eos present producing orange/yellow colored nuclei. Scale bar, 10 μM. (B) Fish were treated without or with neomycin to synchronize hair cell age through hair cell regeneration; then nuclear localized Eos was laser activated in all hair cells and followed over time. The results are graphed for the two pulse-chase hair cell turnover experiments, one without hair cell age synchronization and the other with. Dotted lines represent averages per neuromast ($\pm$ s.d.) of hair cells that were present at the time of Eos protein activation (red) or hair cells generated post-Eos laser activation (green) without neomycin treatment. $N=3$ adult zebrafish, 20 neuromasts. Solid lines represent averages per neuromast ($\pm$ s.d.) of hair cells that were present at the time of Eos protein activation (red) or hair cells generated post-Eos activation (green) with neomycin-induced hair cell age synchronization. $N=3$ adult zebrafish, 17 neuromasts.


Fig. 6. Label retaining support cells are localized to the anterior region of caudal fin neuromasts. (A) Schematic illustrating the orientation of neuromasts in the caudal fin that were analyzed; applies to panels B and C (B) representative z-stack confocal maximum projection image of an adult *Tg(actb2:NLS-Eos)* neuromast following entire neuromast Eos photoactivation (PA) and 6 sequential hair cell regeneration cycles. Scale bar, 10 μM. (C) Diagram illustrating the distribution of label retaining cells using the red fluorescence intensity smooth median regression of 23 overlaid neuromasts. $N=4$ adult zebrafish.

and ventral regions of the neuromast had greatly reduced red Eos fluorescence (Fig. 6A and B). A kernel quantile regression model was performed on the aggregated set to test for significant differences in distribution (Fig. 6C; see Supplemental text for details). Using this analysis, we find distinct support cell populations within neuromasts are identified by label retention. More specifically, our analysis suggests that slowly dividing populations of support cells exist at the anterior–posterior poles

of each neuromast, while support cells in other regions divide more rapidly.

Hair cell precursors are differentially distributed across the neuromast

Label retention studies suggest that support cells in different regions of the neuromast have distinct turnover characteristics
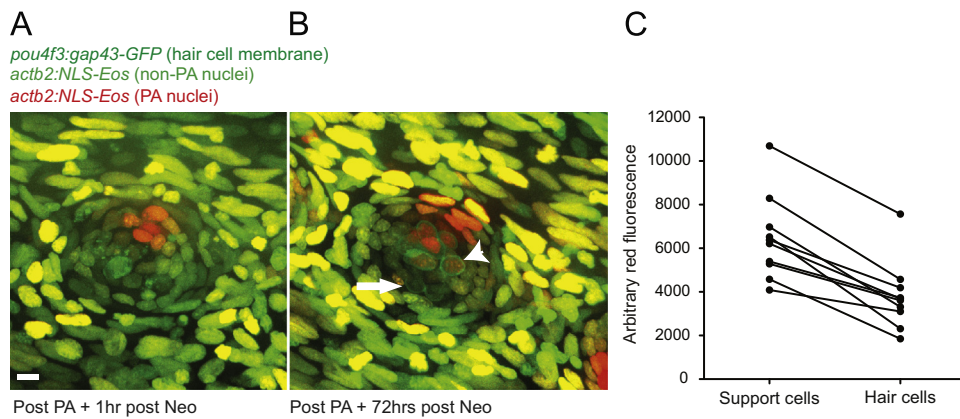
Fig. 7. Selective support cell Eos activation shows non-equitable hair cell contribution during hair cell regeneration. (A) Selective support cells in adult *Tg(pou4f3:gap43-GFP; actb2:NLS-Eos)* caudal neuromasts were activated after neomycin treatment. Arrow indicates surviving hair cell without red nuclei. (B) Hair cell production was traced from labeled support cells during hair cell regeneration. Arrowhead illustrates hair cell with red nuclei produced from support cell with activated red Eos while the arrow illustrates a hair cell with no activated Eos protein. Scale bar, 10 μm. (C) The average red fluorescence of locally activated support cells and regenerated hair cells of 10 different neuromasts following hair cell regeneration.

following multiple rounds of regeneration. We next tested whether support cells in these regions had differential abilities to give rise to new hair cells after a single round of damage. *Tg(actb2:NLS-Eos)* fish were crossed with *Tg(pou4f3:gap43-GFP)* fish to make double transgenic animals we could use to label cell nuclei within neuromasts with Eos photoconversion and identify hair cells with membrane-bound GFP. We photoactivated Eos in approximately 6–8 support cells located in anterior, dorsal, posterior, and ventral quadrants of adult fin ray neuromasts following a single neomycin treatment, and then assessed regenerated hair cells for label after 72 h (Fig. 7A and B). As can bee seen in Fig. 7B, we detect hair cells (denoted by GFP+ membrane) that photoconverted nuclei (arrowheads). We measured the red fluorescence of regenerated hair cells and compared it to red fluorescence in the surrounding activated support cells and found that it was significantly dimmer (Fig. 7C), consistent with the idea that hair cells are derived from dividing precursors and that other support cell divisions are less common. We found no significant difference in the ratio of fluorescence of hair cells to support cells when different quadrants were labeled.

We measured the fraction of total regenerated hair cells that were labeled with photoconverted Eos from each labeled quadrant (Table 1). We found that the chance that support cells produced new hairs cells was equivalent from dorsal, posterior, and ventrally positioned support cells but much less frequent from the anterior quadrant (chi-square test, $p=0.0002$). We also found that cells photoconverted in the anterior quadrant were less likely to give rise to any hair cells (chi-square test, $p=0.03$). These results demonstrate that there are fewer dividing hair cell precursors in the anterior quadrant, a pattern complementary to the distribution of label-retaining compartments in the neuromast.

Discussion

Regeneration of zebrafish lateral line hair cells in larval animals is well established, with dramatic hair cell loss after ototoxin exposure followed by complete hair cell regeneration from proliferating precursors (Williams and Holder, 2000; Harris et al., 2003; Lopez-Schier and Hudspeth, 2006; Hernández et al., 2007; Ma et al., 2008; Wibowo et al., 2011; Mackenzie and Raible, 2012). At these stages, neuromasts have largely completed developmental addition of hair cells and are functionally mature. However, the zebrafish lateral line system undergoes considerable growth

Table 1
Support cells in different quadrants have distinct capacity to generate new hair cells.

Quadrant	Labeled HC	Total HC	Total HC (%)	N	With HC (%)
Anterior	15	139	10.7	15	53.3
Dorsal	35	123	28.5	14	85.7
Posterior	61	229	26.6	25	80.0
Ventral	68	225	30.2	24	91.7

N represents the total number of neuromasts photoconverted. Labeled and total hair cells (HC) are combined across all neuromasts analyzed.

after larval stages with addition of new neuromasts from multiple sources (Nuñez et al., 2009; Wada et al., 2013), and comparable dramatic changes occur throughout many tissues as fish reach adult stages (Parichy et al., 2009). We therefore tested whether hair cell regeneration was possible after growth of the fish was largely complete. We find that adult zebrafish lateral line neuromasts are highly responsive sensory organs that quickly and robustly replace hair cells following aminoglycoside-induced damage, as well as continuously replenishing hair cells undergoing turnover. These results show that adult regeneration is similar to regeneration of lateral line hair cells in larval zebrafish (Williams and Holder, 2000; Harris et al., 2003; Lopez-Schier and Hudspeth, 2006; Hernández et al., 2007; Ma et al., 2008; Wibowo et al., 2011; Mackenzie and Raible, 2012). They complement and extend a recent report examining hair cell recovery in adult zebrafish using gentamicin treatment (Pisano et al., 2014).

Hair cell regeneration continues throughout the life of the zebrafish. In aged animals, we found that hair cell regeneration was complete although somewhat delayed. Zebrafish have the capacity to regenerate many different adult tissues, including fins, heart, nerve, retina, spinal cord and brain (reviewed in Gemberling et al. (2013)). In some tissues regenerative capacity remains robust while in others it declines with age (Itou et al., 2012; Edelmann et al., 2013; Graciarena et al., 2014). Whether there are mechanistic differences in the replacement of lateral line hair cells at different developmental stages is unknown.

Tissues that show a robust regenerative response to damage often exhibit continuous turnover and replacement of cells. Previous reports showed expression of proliferative and cell death markers within larval neuromasts under ambient conditions, consistent with hair cell turnover (Williams and Holder, 2000). However dyes such as acridine orange used to detect cell death are actively taken up by living lateral line hair cells (Santos et al.,

2006) making them an unreliable measure of turnover. Using a *myo6b:NLS-Eos* transgenic line, we observed that in adult zebrafish hair cells undergo continuous homeostatic hair cell death and replacement. This transgenic line allowed us to follow individual neuromasts longitudinally over time without perturbing normal hair cell function or sacrificing the animal for analysis. A potential caveat to this approach is interpreting the loss of photoconverted nuclei as hair cell turnover rather than asymmetric degradation of the red Eos protein within different hair cells of labeled neuromasts. This appears unlikely, since we observed similar kinetics of hair cell turnover and replacement using a conventional BrdU pulse-chase paradigm. We and others detect little change in the high fluorescence levels of red Eos months after photoactivation in other cell types (our unpublished observations; McMenamin et al., 2014). It is possible that the nuclear localization of the NLS-Eos protein protects it from degradation, which may make it amendable to other long-term cell labeling experiments.

The stability of photoconverted NLS-Eos allowed us to conduct a modified label-retention assay, often used to identify slow cycling progenitor populations. It shares some advantages with methods using labeled histones (Tumbar et al., 2004; Foudi et al., 2009) as it does not require BrdU incorporation during S-phase. We found that support cells in the anterior pole of caudal fin neuromasts, and to some degree in the posterior pole, retained higher levels of activated Eos after many rounds of induced proliferation from hair cell damage and regeneration. We note that we have identified these label-retaining compartments within the neuromasts of the caudal fin, where hair cells are polarized along the anterior–posterior axis. It would be interesting to know whether the location of the label-retaining compartments always corresponds with neuromast hair cell polarity, for example whether the compartment is rotated in neuromasts whose hair cells have dorsoventral polarity. Rapidly-dividing hair cell precursors have been described previously to divide in polarized compartments that are perpendicular with respect to hair cell polarization (Wibowo et al., 2011; Mirkovic et al., 2012), consistent with our observations that these compartments are less likely to retain label. We had previously noted that peripheral supports cells labeled with BrdU at a lower frequency and with different kinetics than more centrally-located cells but did not note orientation with respect to neuromast polarity (Ma et al., 2008). These results are consistent with our observations that label-retaining cells are more prevalent at peripheral locations.

Although Eos lineage tracing is a useful tool in marking and tracking cells, it is not without its limitations. First, the amount of Eos protein that can be photoconverted in each cell at a given time is finite; this limits the number of cell divisions through which progeny can be tracked, given that each cell division reduces the fluorescence by at least half. We are not able to detect red fluorescence above background after any more than two cell divisions. Another problem arises with the density and sizes of cells within a given tissue. Eos is not photoconvertible with two-photon microscopy using current schemes. If the cells are small and tightly packed, such as it is within the neuromasts, labeling single cells is extremely difficult and usually is not achieved without inadvertently activating Eos in other cells due to light scatter.

Time-lapse studies of hair cell regeneration in larval zebrafish show that pairs of hair cells are produced from symmetric divisions of underlying support cells in a mechanism proposed to maintain hair cell polarity (López-Schier and Hudspeth, 2006; Wibowo et al., 2011; Mirkovic et al., 2012). These results suggest that continual hair cell production would eventually deplete hair cell precursors if no system were present to restore them. Both our Eos photoactivation cell-lineage assay and BrdU incorporation studies support the idea that regenerating adult lateral line hair cells are also derived from division of underlying support cells. We

also did not observe an overall depletion of support cells after multiple hair cell regeneration cycles, indicating that support cells that act as hair cell precursors are replaced.

While the source of replacement hair cell precursors remains unresolved, we speculate that these cells may come from the slower-dividing label-retaining populations that predominate in the anterior quadrant of neuromasts. Preliminary Eos lineage tracing experiments suggest that some cells move from this zone towards the center where they can act as hair cell precursors (IAC, unpublished results). However, the limits of Eos protein detection through multiple rounds of division (noted above) prevent a systematic analysis of cell lineage to the level needed to definitively identify the source(s) of progenitors. While previous analysis of regeneration in larval zebrafish demonstrates pairs of hair cells arise from symmetrically dividing precursors, it is possible that hair cells are also produced by asymmetric divisions in adults. Hair cell precursors themselves may also be generated by symmetric or asymmetric divisions. We cannot delineate whether support cells are dividing symmetrically or asymmetrically using the label-retaining assay, and can only conclude that label-retaining cells divide less frequently. Cell lineage and extended time-lapse studies, perhaps with indelible lineage tracing techniques using Cre-based methods, need to be conducted to distinguish amongst these possibilities.

Mammalian tissues, like the skin, blood, and intestine that have continuous cellular turnover (reviewed in Fliedner (1998), Fuchs (2009), Hsu et al. (2014), Tan and Barker (2014), Clevers et al. (2014)) and high regenerative capability have been shown to have resident stem cell populations in distinct stem cell niches (see Barker et al. (2010), Tan and Barker (2014), Clevers et al. (2014), Rezza et al. (2014) for reviews). It is thought that these secluded regions provide a regulated microenvironment that maintains stem cells in a more pluripotent or quiescent state. We speculate that the label retaining population within the neuromast may reside within a distinct niche. Label-retaining support cells are found on the periphery and adjacent to interneuromast cell populations that act as a source of de novo neuromast generation (Grant et al., 2005). A possible function of these adult caudal fin interneuromast cells is to provide instructive cues to adjacent support cells to maintain some support cells in a more quiescent state, or function as a hub to give support cells cellular/tissue polarity. Performing laser ablation experiments will help better understanding their role in neuromast maintenance.

During postembryonic stages Wnt signaling instruct neuromasts to become organized into stitches with new neuromasts formed from cells migrating from the edge of existing neuromasts (Wada et al., 2013). In addition, during fin regeneration new fin ray lines form from a new primordium generated from the last remaining neuromast adjacent to the amputation site (Dufourcq et al., 2006). It is tempting to speculate that these new neuromasts arise from the same peripheral support cell pool that might repopulate hair cell precursors after turnover or regeneration. Besides Wnt, other regulators of larval neuromast maintenance have begun to be elucidated, including Notch and Jak-Stat signals (Ma et al., 2008; Wibowo et al., 2011; Liang et al., 2012; Head et al., 2013; Wada et al., 2013; Jacques et al., 2014; Jiang et al., 2014; Steiner et al., 2014). Whether these signals continue to be used during adult stages remains to be determined.

Sensory hair cell regeneration occurs in all vertebrates examined except mammals (see Brignull et al. (2009) for review). In the inner ear, hair cells are regenerated from symmetric (Raphael, 1992; Tsue et al., 1994; Stone and Rubel, 2000) and asymmetric (Roberson et al., 1992; Stone et al., 1999; Stone and Rubel, 2000) support cell divisions, as well as through direct-phenotypic conversions (Jones and Corwin, 1996; Adler and Raphael, 1996; Baird et al., 1996, 2000; Roberson et al., 2004; Taylor and Forge, 2005;

Duncan et al., 2006; Cafaro et al., 2007). By contrast regeneration in the lateral line of zebrafish larvae is largely through proliferation of precursors (Wibowo et al., 2011; Mackenzie and Raible, 2012). Like the lateral line system, the avian vestibular epithelium also shows continuous hair cell turnover (Jørgensen and Mathiesen, 1988; Roberson et al., 1992; Kil et al., 1997). It may be that zebrafish lateral line hair cell regeneration is simply redirecting mechanisms present for ongoing hair cell production that are greatly accelerated during massive hair cell loss due to trauma. Regardless of the mechanisms underlying replacement of lost hair cells, a system must exist to replenish support cells that are used to regenerate hair cells. To what degree mechanisms of hair cell regeneration are conserved across species remains to be determined.

Regeneration is a necessary and fundamental biological process that varies greatly amongst species. Mammals have a very restricted ability to regenerate when compared to cold-blooded vertebrates. The ability to restore damaged or lost tissue also decreases over the lifespan of most animals. It is encouraging to see that not only can zebrafish regenerate lateral line hair cells after multiple hair cell ablations, but also that they can regenerate hair cells as adults. Our results indicate that there are at least two distinct support cell populations within lateral line neuromasts. One population of support cells promptly gives rise to lateral line hair cells following hair cell ablation, while the other is a label retaining support cell population that is less mitotically active. Understanding the different environmental cues zebrafish support cells are exposed to during hair cell regeneration and hair cell maintenance may prove a crucial step in decoding and promoting hair cell and support cell regeneration in humans.

Materials and methods

Zebrafish strains and maintenance

Adult zebrafish were maintained at 28.5 °C. sqet20Et was a gift from Korzh (Parinov et al., 2004).Tg(pou4f3:gap43-GFP) was a gift from Baier and previously described in Xiao et al. (2005). To generate Tg(Ca-tuba1a:tdTomato), a Carassius auratus alpha-1-tubulin fragment containing 1696 bp of 5' flanking sequence (Goldman et al., 2001) was fused in frame to the tdTomato sequence, flanked by two I-SceI meganuclease recognition sites in the pBluescript vector. Linearized DNA containing this construct was co-injected with the I-SceI meganuclease enzyme into one-cell stage zebrafish embryos (Thermes et al., 2002). The myo6b promoter was previously described in Obholzer et al. (2008). Tg (actb2:NLS-Eos) fish were created using the Gateway system as previously described in (Kwan et al., 2007). All procedures were approved by the University of Washington Institutional Animal Care and Use Committee.

Neomycin

Neomycin sulfate (Sigma, St. Louis, MO) was diluted in E3 embryo media (14.97 mM NaCl, 500 μM KCl, 42 μM Na$_2$HPO$_4$, 150 μM KH$_2$PO$_4$, 1 mM CaCl$_2$ dehydrate, 1 mM MgSO$_4$, and 0.714 mM NaHCO$_3$) to a final concentration of 400 μM. All adult zebrafish hair cell ablations were carried out in 400 μM neomycin for 1 h followed by a 1 h recovery period in E3 media at 28.5 °C. Hair cells were scored before neomycin, 2 and 72 h after treatment, and then repeated as indicated in the experiment. Sibling fish were used as controls and were mock-treated by handling and relocating to drug-free media.

Adult zebrafish hair cell and support cell labeling

Adult zebrafish immunohistochemistry was performed as described in Ma et al. (2008).Tg(pou4f3:gap43-GFP) hair cells were stained using rabbit anti-GFP primary antibodies and Alexa 488-conjugated anti-rabbit secondary (1:500; Molecular Probes). Support cells were visualized using the pan-nuclear stain SYTOX green (1:10,000; Molecular Probes).

Live hair cell regeneration counts were conducted in adult zebrafish submerged in E3 containing 0.2% buffered MESAB (MS-222; ethyl-m-aminobenzoate methanesulphonate) under epi-fluorescence using a 63× water objective on a Zeiss Axioplan 2 microscope. Support cell confocal images were taken on a Zeiss LSM 5 Pa confocal microscope. Hair cell and support cell counts were recorded from all the neuromasts of the caudal peduncle stitch, with a minimum of 9 neuromasts per fish and 4 fish per treatment. Whole images were processed using the Pascal software, ImageJ, and Adobe Photoshop CS4.

Adult zebrafish mitotic cell labeling

Adult zebrafish were incubated in 10 mM of bromodeoxyuridine (BrdU; Sigma) in E3 embryo media solution containing 1% dimethyl sulfoxide (DMSO) 12 h after neomycin treatment for 24 h and then fixed and stained 48 h, 6 days, and 12 days post-BrdU incubation. BrdU immunohistochemistry was performed as described in Ma et al. (2008): hair cells were labeled with mouse anti-parvalbumin primary antibodies and Alexa 488-conjugated anti-mouse secondary antibodies (1:500; Molecular Probes), and BrdU+ cells were labeled with rat anti-BrdU primary antibodies and Alexa 568-conjugated anti-rat secondary antibodies (1:200; Molecular Probes).

Graphs and statistical analysis were carried out in Graphpad Prism.

Eos photoactivation and imaging

Adult zebrafish were anesthetized and placed into 6-mL chambers with the caudal fin stabilized with a sponge. Chambers were placed on an inverted Axio Observer D1 spinning disk system (Intelligent Imaging Innovations) equipped with an Evolve 10 MHz EMCCD camera (Photometrics) and a Zeiss C-Apochromat 63×/1.2 NA water objective. Camera intensification was set to 500, and 488 nm and 561 nm exposure times were adjusted to maintain maximum intensities below fluorescence saturation.

Photoactivation of green Eos protein was performed on Tg (myo6b:NLS-Eos) and double transgenic Tg(bactin2:NLS-Eos;pou4f3: gap43-GFP) fish by targeting a 405 nm laser through the 63× objective for three 10 ms pulse exposures. Nuclei in neuromasts are easily distinguished from surrounding epidermal tissue by their smaller size and circumferential orientation.

Red Eos fluorescence analysis

For hair cell turnover, thresholding was established by creating Z-stack images of all photoconverted neuromasts and three non-photoconverted neuromasts for each fish. Maximum intensity projections were created for photoactivated and non-photo-activated neuromast Z-stacks. To determine the lower threshold for hair cell Eos activation, the basal red intensity levels and the standard deviations of the three non-photoconverted neuromasts were measured, averaged, and added with 2× the averaged standard deviations. (avg. red fluorescence from 3 non-activated neuromasts)+2(avg. s.d. red fluorescence from non-activated neuromasts)=lower threshold for Eos activation. Slidebook

software was used for image analysis and Adobe Photoshop CS4 was used for figure production.

For label retention experiments, the position and red fluorescence of all nuclei of activated fin neuromasts were measured after 6 sequential neomycin treatments using ImageJ cell counter software. To compare all neuromasts to each other, neuromasts were aligned along the anterior–posterior axis and this diameter length was set to 1. All Cartesian coordinates were measured relative to this axis and then converted to polar coordinates. The red fluorescence was normalized to the cell with the highest red fluorescence intensity in each neuromast. 23 Neuromasts were aligned and stacked on top of each other to get a distribution frequency. The median fluorescence regression diagram was created as described in the Supplemental text (Figs. S1–S4).

For the cell lineage tracing experiments, regions of interest were created using Slidebook software to selectively photoactivate Eos in subsets of support cells in predetermined regions of caudal fin neuromasts. Fish were treated with neomycin to ablate hair cells and induce support cell divisions. The red and green fluorescence levels were measured for all the hair cells of activated neuromasts. The red-to-green fluorescence ratio was calculated for every hair cell and then plotted as a frequency histogram. Cells that had a ratio of 0.8 or higher were considered hair cells with activated Eos.

Authors contributions

Ivan Cruz designed and performed experiments, data analysis and manuscript preparation. Ryan Kappedal conducted statistical analysis for the label retaining cell experiment. Trevor Hoffman and Thomas Schilling generated the *Tg(Ca-tuba1a:tdTomato)* transgenic line. Scott Mackenzie generated the *Tg(actb2:NLS-Eos)* fish line. Dale Hailey generated the *Tg(myo6b:NLS-Eos)* line and assisted with photoactivation studies. David Raible designed experiments, performed analysis and prepared the manuscript.

Acknowledgments

Appendix A. Supplementary material

Supplementary data associated with this article can be found in the online version at doi:10.1016/j.ydbio.2015.03.019.

References

Adler, H.J., Raphael, Y., 1996. New hair cells arise from supporting cell conversion in the acoustically damaged chick inner ear. Neurosci. Lett. 205 (1), 17–20.
Baird, R.A., Steyger, P.S., Schuff, N.R., 1996. Mitotic and nonmitotic hair cell regeneration in the bullfrog vestibular otolith organs. Ann. N. Y. Acad. Sci. 781, 59–70.
Baird, R.A., Burton, M.D., Lysakowski, A., Fashena, D.S., Naeger, R.A., 2000. Hair cell recovery in mitotically blocked cultures of the bullfrog saccule. Proc. Natl. Acad. Sci. USA 97 (22), 11722–11729.
Barker, N., Bartfeld, S., Clevers, H., 2010. Tissue-resident adult stem cell populations of rapidly self-renewing organs. Cell Stem Cell 7 (6), 656–670.
Brigande, J.V., Heller, S., 2009. Quo vadis, hair cell regeneration? Nat. Neurosci. 6, 679–685.
Brignull, H.R., Raible, D.W., Stone, J.S., 2009. Feathers and fins: non-mammalian models for hair cell regeneration. Brain Res. 1277, 12–23.
Cafaro, J., Lee, G.S., Stone, J.S., 2007. Atoh1 expression defines activated progenitors and differentiating hair cells during avian hair cell regeneration. Dev. Dyn. 236 (1), 156–170.
Clevers, H., Loh, K.M., Nusse, R., 2014. Stem cell signaling – an integral program for tissue renewal and regeneration: Wnt signaling and stem cell control. Science 346 (6205), 1248012.
Dufourcq, P., Roussigné, M., Blader, P., Rosa, F., Peyrieras, N., Vriz, S., 2006. Mechanosensory organ regeneration in adults: the zebrafish lateral line as a model. Mol. Cell Neurosci. 33 (2), 180–187.
Duncan, L.J., Mangiardi, D.A., Matsui, J.I., Anderson, J.K., McLaughlin-Williamson, K., Cotanche, D.A., 2006. Differential expression of unconventional myosins in apoptotic and regenerating chick hair cellsconfirms two regeneration mechanisms. J. Comp. Neurol. 499 (5), 691–701.
Edelmann, K., Glashauser, L., Sprungala, S., Hesl, B., Fritschle, M., Ninkovic, J., Godinho, L., Chapouton, P., 2013. Increased radial glia quiescence, decreased reactivation upon injury and unaltered neuroblast behavior underlie decreased neurogenesis in the aging zebrafish telencephalon. J. Comp. Neurol. 521 (13), 3099–3115.
Fior, J., 2014. Salamander regeneration as a model for developing novel regenerative and anticancer therapies. J. Cancer 5 (8), 715–719.
Fliedner, T.M., 1998. The role of blood stem cells in hematopoietic cell renewal. Stem Cells 16, 361–374.
Foudi, A., Hochedlinger, K., Van Buren, D., Schindler, J.W., Jaenisch, R., Carey, V., Hock, H., 2009. Analysis of histone 2B GFP retention reveals slowly cycling hematopoietic stem cells. Nat. Biotechnol. 27 (1), 84–90.
Fuchs, E., 2009. The tortoise and the hair: slow-cycling cells in the stem cell race. Cell 137 (5), 811–819.
Gemberling, M., Bailey, T.J., Hyde, D.R., Poss, K.D., 2013. The zebrafish as a model for complex tissue regeneration. Trends Genet. 29 (11), 611–620.
Goldman, D., Hankin, M., Li, Z., Dai, X., Ding, J., 2001. Transgenic zebrafish for studying nervous system development and regeneration. Transgenic Res. 10, 21–33.
Graciarena, M., Dambly-Chaudière, C., Ghysen, A., 2014. Dynamics of axonal regeneration in adult and aging zebrafish reveal the promoting effect of a first lesion. Proc. Natl. Acad. Sci. USA 111 (4), 1610–1615.
Grant, K.A., Raible, D.W., Piotrowski, T., 2005. Regulation of latent sensory hair cell precursors by glia in the zebrafish lateral line. Neuron 45 (1), 69–80.
Harris, J.A., Cheng, A.G., Cunningham, L.L., MacDonald, G., Raible, D.W., Rubel, E.W., 2003. Neomycin-induced hair cell death and rapid regeneration in the lateral line of zebrafish (Danio rerio). J. Assoc. Res. Otolaryngol. 4 (2), 219–234.
Hawkins, N.M., Atha, J., 1976. A study of passenger behaviour on a slow speed travellator system. Ergonomics 4, 499–517.
Head, J.R., Gacioch, L., Pennisi, M., Meyers, J.R., 2013. Activation of canonical Wnt/β-catenin signaling stimulates proliferation in neuromasts in the zebrafish posterior lateral line. Dev. Dyn. 242 (7), 832–846.
Hernández, P.P., Olivari, F.A., Sarrazin, A.F., Sandoval, P.C., Allende, M.L., 2007. Regeneration in zebrafish lateral line neuromasts: expression of the neural progenitor cell marker sox2 and proliferation-dependent and -independent mechanisms of hair cell renewal. Dev. Neurobiol. 67 (5), 637–654.
Hsu, Y.C., Li, L., Fuchs, E., 2014. Emerging interactions between skin stem cells and their niches. Nat. Med. 20 (8), 847–856.
Itou, J., Kawakami, H., Burgoyne, T., Kawakami, Y., 2012. Life-long preservation of the regenerative capacity in the fin and heart in zebrafish. Biol. Open 1 (8), 739–746.
Jacques, B.E., Montgomery 4th, W.H., Uribe, P.M., Yatteau, A., Asuncion, J.D., Resendiz, G., Matsui, J.I., Dabdoub, A., 2014. The role of Wnt/β-catenin signaling in proliferation and regeneration of the developing basilar papilla and lateral line. Dev. Neurobiol. 74 (4), 438–456.
Jiang, L., Romero-Carvajal, A., Haug, J.S., Seidel, C.W., Piotrowski, T., 2014. Gene-expression analysis of hair cell regeneration in the zebrafish lateral line. Proc. Natl. Acad. Sci. USA 111 (14), E1383–E1392.
Jones, J.E., Corwin, J.T., 1996. Regeneration of sensory cells after laser ablation in the lateral line system: hair cell lineage and macrophage behavior revealed by time-lapse video microscopy. J. Neurosci. 16 (2), 649–662.
Jørgensen, J.M., Mathiesen, C., 1988. The avian inner ear. Continuous production of hair cells in vestibular sensory organs, but not in the auditory papilla. Naturwissenschaften 75 (6), 319–320.
Kil, J., Warchol, M.E., Corwin, J.T., 1997. Cell death, cell proliferation, and estimates of hair cell life spans in the vestibular organs of chicks. Hear. Res. 114 (1–2), 117–126.
Kwan, K.M., Fujimoto, E., Grabher, C., Mangum, B.D., Hardy, M.E., Campbell, D.S., Parant, J.M., Yost, H.J., Kanki, J.P., Chien, C.B., 2007. The Tol2kit: a multisite gateway-based construction kit for Tol2 transposon transgenesis constructs. Dev. Dyn. 236 (11), 3088–3099.
Liang, J., Wang, D., Renaud, G., Wolfsberg, T.G., Wilson, A.F., Burgess, S.M., 2012. The stat3/socs3a pathway is a key regulator of hair cell regeneration in zebrafish. J. Neurosci. 32 (31), 10662–10673.
López-Schier, H., Hudspeth, A.J., 2006. A two-step mechanism underlies the planar polarization of regenerating sensory hair cells. Proc. Natl. Acad. Sci. USA 103 (49), 18615–18620.
Ma, E.Y., Rubel, E.W., Raible, D.W., 2008. Notch signaling regulates the extent of hair cell regeneration in the zebrafish lateral line. J. Neurosci. 28 (9), 2261–2273.
Mackenzie, S.M., Raible, D.W., 2012. Proliferative regeneration of zebrafish lateral line hair cells after different ototoxic insults. PLoS One 7 (10), e47257.
McMenamin, S.K., Bain, E.J., McCann, A.E., Patterson, L.B., Eom, D.S., Waller, Z.P., Hamill, J.C., Kuhlman, J.A., Eisen, J.S., Parichy, D.M., 2014. Thyroid hormone-dependent adult pigment cell lineage and pattern in zebrafish. Science 345 (6202), 1358–1361.

Mirkovic, I., Pylawka, S., Hudspeth, A.J., 2012. Rearrangements between differentiating hair cells coordinate planar polarity and the establishment of mirror symmetry in lateral-line neuromasts. Biol. Open 1 (5), 498–505.

Nicolson, T., 2005. The genetics of hearing and balance in zebrafish. Annu. Rev. Genet. 39, 9–22.

Nuñez, V.A., Sarrazin, A.F., Cubedo, N., Allende, M.L., Dambly-Chaudière, C., Ghysen, A., 2009. Postembryonic development of the posterior lateral line in the zebrafish. Evol. Dev. 11 (4), 391–404.

Obholzer, N., Wolfson, S., Trapani, J.G., Mo, W., Nechiporuk, A., Busch-Nentwich, E., Seiler, C., Sidi, S., Söllner, C., Duncan, R.N., Boehland, A., Nicolson, T., 2008. Vesicular glutamate transporter 3 is required for synaptic transmission in zebrafish hair cells. J. Neurosci. 28 (9), 2110–2118.

Ou, H.C., Raible, D.W., Rubel, E.W., 2007. Cisplatin-induced hair cell loss in zebrafish (Danio rerio) lateral line. Hear. Res. 233 (1–2), 46–53.

Parichy, D.M., Elizondo, M.R., Mills, M.G., Gordon, T.N., Engeszer, R.E., 2009. Normal table of postembryonic zebrafish development: staging by externally visible anatomy of the living fish. Dev. Dyn. 238 (12), 2975–3015.

Parinov, S., Kondrichin, I., Korzh, V., Emelyanov, A., 2004. Tol2 transposon-mediated enhancer trap to identify developmentally regulated zebrafish genes in vivo. Dev. Dyn. 231 (2), 449–459.

Pisano, G.C., Mason, S.M., Dhliwayo, N., Intine, R.V., Sarras Jr., M.P., 2014. An assay for lateral line regeneration in adult zebrafish. J. Vis. Exp. (86), e51343. http://dx.doi.org/10.3791/51343.

Rando, T.A., Wyss-Coray, T., 2014. Stem cells as vehicles for youthful regeneration of aged tissues. J. Gerontol. A Biol. Sci. Med. Sci. 69 (S1), S39–S42.

Raphael, Y., 1992. Evidence for supporting cell mitosis in response to acoustic trauma in the avian inner ear. J. Neurocytol. 21 (9), 663–671.

Raphael, Y., Lenoir, M., Wroblewski, R., Pujol, R., 1991. The sensory epithelium and its innervation in the mole rat cochlea. J. Comp. Neurol. 314 (2), 367–382.

Rezza, A., Sennett, R., Rendl, M., 2014. Adult stem cell niches: cellular and molecular components. Curr. Top. Dev. Biol. 107, 333–372.

Roberson, D.W., Alosi, J.A., Cotanche, D.A., 2004. Direct transdifferentiation gives rise to the earliest new hair cells in regenerating avian auditory epithelium. J. Neurosci. Res. 78 (4), 461–471.

Roberson, D.F., Weisleder, P., Bohrer, P.S., Rubel, E.W., 1992. Ongoing production of sensory cells in the vestibular epithelium of the chick. Hear. Res. 57 (2), 166–174.

Santos, F., MacDonald, G., Rubel, E.W., Raible, D.W., 2006. Lateral line hair cell maturation is a determinant of aminoglycoside susceptibility in zebrafish (Danio rerio). Hear. Res. 213 (1–2), 25–33.

Simon, A., Tanaka, E.M., 2013. Limb regeneration. WIREs Dev. Biol. 2 (2), 291–300.

Song, J., Yan, H.Y., Popper, A.N., 1995. Damage and recovery of hair cells in fish canal (but not superficial) neuromasts after gentamicin exposure. Hear. Res. 91 (1–2), 63–71.

Sousounis, K., Baddour, J.A., Tsonis, P.A., 2014. Aging and regeneration in vertebrates. Curr. Top. Dev. Biol. 108, 217–246.

Steiner, A.B., Kim, T., Cabot, V., Hudspeth, A.J., 2014. Dynamic gene expression by putative hair-cell progenitors during regeneration in the zebrafish lateral line. Proc. Natl. Acad. Sci. USA 111 (14), E1393–E1401.

Stone, J.S., Rubel, E.W., 2000. Cellular studies of auditory hair cell regeneration in birds. Proc. Natl. Acad. Sci. USA 97 (22), 11714–11721.

Stone, J.S., Choi, Y.S., Woolley, S.M., Yamashita, H., Rubel, E.W., 1999. Progenitor cell cycling during hair cell regeneration in the vestibular and auditory epithelia of the chick. J. Neurocytol. 28 (10–11), 863–876.

Tan, D.W., Barker, N., 2014. Intestinal stem cells and their defining niche. Curr. Top. Dev. Biol. 107, 77–107.

Taylor, R.R., Forge, A., 2005. Hair cell regeneration in sensory epithelia from the inner ear of a urodele amphibian. J. Comp. Neurol. 484 (1), 105–120.

Tetteh, P.W., Farin, H.F., Clevers, H., 2014. Plasticity within stem cell hierarchies in mammalian epithelia. Trends Cell Biol. S0962–8924 (14), 00161–00165.

Thermes, V., Grabher, C., Ristoratore, F., Bourrat, F., Choulika, A., Wittbrodt, J., Joly, J.S., 2002. I-SceI meganuclease mediates highly efficient transgenesis in fish. Mech. Dev. 118, 91–98.

Thomas, E.D., Cruz, I.A., Hailey, D.W., Raible, D.W., 2015. There and back again: development and regeneration of the zebrafish lateral line system. WIREs Dev. Biol. 10, 1002. http://dx.doi.org/10.1002/wdev.160.

Ton, C., Parng, C., 2005. The use of zebrafish for assessing ototoxic and otoprotective agents. Hear. Res. 208 (1–2), 79–88.

Tsue, T.T., Watling, D.L., Weisleder, P., Coltrera, M.D., Rubel, E.W., 1994. Identification of hair cell progenitors and intermitotic migration of their nuclei in the normal and regenerating avian inner ear. J. Neurosci. 14 (1), 140–152.

Tumbar, T., Guasch, G., Greco, V., Blanpain, C., Lowry, W.E., Rendl, M., Fuchs, E., 2004. Defining the epithelial stem cell niche in skin. Science 303 (5656), 359–363.

Wada, H., Ghysen, A., Asakawa, K., Abe, G., Ishitani, T., Kawakami, K., 2013. Wnt/Dkk negative feedback regulates sensory organ size in zebrafish. Curr. Biol. 23 (16), 1559–1565.

Whitfield, T.T., 2002. Zebrafish as a model for hearing and deafness. J. Neurobiol. 53 (2), 157–171.

Wibowo, I., Pinto-Teixeira, F., Satou, C., Higashijima, S., López-Schier, H., 2011. Compartmentalized Notch signaling sustains epithelial mirror symmetry. Development 138 (6), 1143–1152.

Williams, J.A., Holder, N., 2000. Cell turnover in neuromasts of zebrafish larvae. Hear. Res. 143 (1–2), 171–181.

Xiao, T., Roeser, T., Staub, W., Baier, H., 2005. A GFP-based genetic screen reveals mutations that disrupt the architecture of the zebrafish retinotectal projection. Development 132 (13), 2955–2967.